crystals

Article

A Standard Structure for Bile Acids and Derivatives

Francisco Meijide [1,*], Santiago de Frutos [1], Victor H. Soto [2], Aida Jover [1], Julio A. Seijas [3], María Pilar Vázquez-Tato [3], Francisco Fraga [4] and José Vázquez Tato [1]

1 Departamento de Química Física, Facultad de Ciencias, Universidad de Santiago de Compostela, Avda. Alfonso X El Sabio s/n, 27002 Lugo, Spain; santiagodefrutos@hotmail.com (S.d.F.); aida.jover@usc.es (A.J.); jose.vazquez@usc.es (J.V.T.)

2 Escuela de Química, Centro de Investigación en Electroquímica y Energía Química (CELEQ), Universidad de Costa Rica, 11501-2060 San José, Costa Rica; vsototellinie@gmail.com

3 Departamento de Química Orgánica, Facultad de Ciencias, Universidad de Santiago de Compostela, Avda. Alfonso X El Sabio s/n, 27002 Lugo, Spain; julioa.seijas@usc.es (J.A.S.); pilar.vazquez.tato@usc.es (M.P.V.-T.)

4 Departamento de Física Aplicada, Facultad de Ciencias, Universidad de Santiago de Compostela, Avda. Alfonso X El Sabio s/n, 27002 Lugo, Spain; francisco.fraga@usc.es

* Correspondence: francisco.meijide@usc.es

Received: 22 December 2017; Accepted: 1 February 2018; Published: 6 February 2018

Abstract: The crystal structures of two ester compounds (a monomer in its methyl ester form, with an amino isophthalic group, and a dimer in which the two steroid units are linked by a urea bridge recrystallized from ethyl acetate/methanol) derived from cholic acid are described. Average bond lengths and bond angles from the crystal structures of 26 monomers and four dimers (some of them in several solvents) of bile acids and esters (and derivatives) are used for proposing a standard steroid nucleus. The hydrogen bond network and conformation of the lateral chain are also discussed. This standard structure was used to compare with the structures of both progesterone and cholesterol.

Keywords: crystal structure; steroid; bile acids

1. Introduction

Bile salts (BS) are important biological surfactants, which play crucial roles in several processes of vertebrates [1,2]. The chemical structure of the most important BS in mammals involves the hydrophobic and rigid cyclopentanoperhydrophenanthrene nucleus (also characteristic of cholesterol) bearing one, two, or three hydroxy groups at positions 3, 7, and 12, as well as an isopentanoic lateral chain. The hydroxy group at position 3 is considered as the head of the molecule, and the carboxylic group its tail. Bile acids (BA) are compounds resulting from the protonation of the carboxylate group of BS, and can be conjugated with the amino acids glycine and taurine. Those corresponding to cholic (CA, **1**, Table 1), lithocholic (**2**), deoxycholic (DCA, **3**), chenodeoxycholic (**7**), and ursodeoxycholic (**8**) acids are among the most important and studied BA. The orientation of the OH substituents is such that BS are facially amphipathic molecules with three-axial chirality [3] that self-aggregate in aqueous solution, forming aggregates, which usually have low aggregation numbers [4,5].

Table 1. Chemical structure and numbering of the bile acids ($R_4 = CO_2H$), bile acid esters ($R_4 = CO_2CH_3$), and 24-amino derivatives ($R_4 = NH_2$) reviewed in this paper.

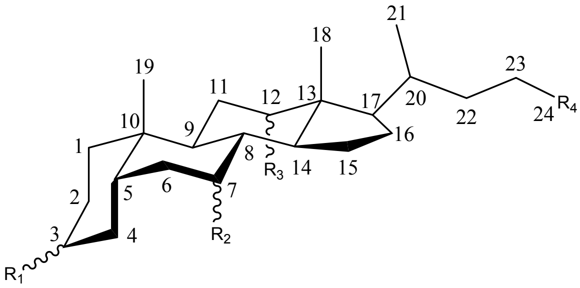

R_1	R_2	R_3	R_4	Compound	Reference
α-OH	α-OH	α-OH	CO_2H	**1**	[6]
α-OH	H	H	CO_2H	**2**	[7]
α-OH	H	α-OH	CO_2H	**3**	[8]
α-OH	H	β-OH	CO_2H	**4**	[8]
β-OH	H	β-OH	CO_2H	**5**	[8]
β-OH	H	α-OH	CO_2H	**6**	[9]
α-OH	α-OH	H	CO_2H	**7**	[10]
α-OH	β-OH	H	CO_2H	**8**	[10]
β-OH	α-OH	H	CO_2H	**9**	[10]
β-OH	β-OH	H	CO_2H	**10**	[10]
=O	H	α-OH	CO_2H	**11**	[8]
β-NH_2	α-OH	α-OH	CO_2H	**12**	[11]
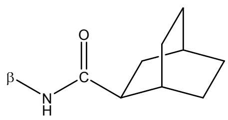	α-OH	α-OH	CO_2H	**13**	[12]
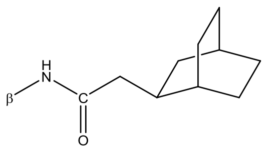	α-OH	α-OH	CO_2H	**14**	[13]
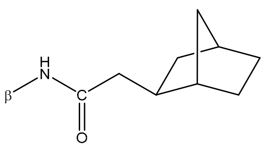	α-OH	α-OH	CO_2H	**15**	[14]
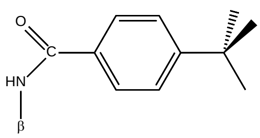	α-OH	α-OH	CO_2H	**16**	[15]
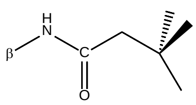	α-OH	α-OH	CO_2H	**17**	See Supplementary Materials

Table 1. *Cont.*

R_1	R_2	R_3	R_4	Compound	Reference
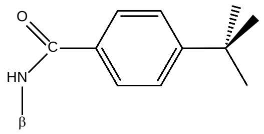	α-OH	H	CO_2H	**18**	[16]
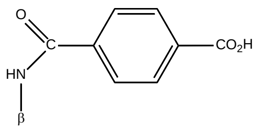	α-OH	α-OH	CO_2H	**19**	See Supplementary Materials
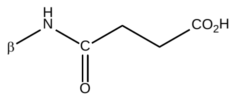	α-OH	α-OH	CO_2H	**20**	[17]
α-OH	α-OH	α-OH	NH_2	**21**	[11]
α-OH	α-OH	H	NH_2	**22**	[11]
β-N_3	α-OH	α-OH	CO_2CH_3	**23**	See Supplementary Materials
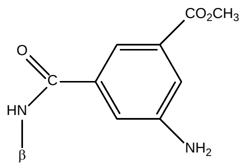	α-OH	α-OH	CO_2CH_3	**24**	this paper
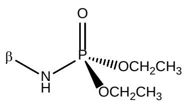	α-OH	α-OH	CO_2CH_3	**25**	See Supplementary Materials
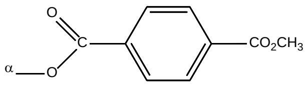	α-OH	α-OH	CO_2CH_3	**26**	See Supplementary Materials

Modifications of the functional groups lead to a great number of BS derivatives, some naturally-occurring. For example, typical modifications of the terminal carboxylic acid group are ester (BE) and amide derivatives, while keto and amine groups are common modifications of the hydroxy groups. A variety of groups of different natures have also been linked to the steroid nucleus at the hydroxy group locations, mainly through ester and amide bonds. Compounds obtained by substitution at C3 have been particularly useful. Examples are derivatives with hydrophobic and bulky substituents (*t*-buthylphenyl, naphthyl, adamantyl), saccharides (mannose), and amino acids (tryptophan). In aqueous solution they behave as surfactants, the aggregates showing a wide range of structures. The subject has been reviewed recently [18]. On the other hand, the head–tail structure of BS allows the synthesis of head-to-head [19], head-to-tail [20], and tail-to-tail [21] dimers.

The ratio of number of steroid groups to number of charged groups (equal to 1 in natural BS) can be easily modified for monomers, dimers, and oligomers. Consequently, the hydrophobic–hydrophilic balance of the compound is either increased or reduced, thus modifying its self-aggregation in aqueous solution. Several papers dealing with the physicochemical properties and applications in fields such as supramolecular chemistry, biomedicine, and pharmaceutics have been reported [18,22–28].

The characterization of the crystal structures of BS and BA by X-ray analysis has been a topic of interest [29,30]. This knowledge can be very useful for the proposition of the structure of BS aggregates in aqueous solution, a strategy firstly and largely employed by Giglio and coworkers [31], and of the supramolecular structures of BS derivatives [32]. Miyata et al. [33–36] have carried out studies on BA crystals in a large variety of solvents and guests, also systematically modified the steroid structure. It can be concluded from these studies that the solid state structure depends on subtle differences in donor–acceptor relationships among the hydrogen bonding groups of guest and steroid molecules. The solution of the crystal structures of the four 3,12-dihydroxy epimers of DCA was used to successfully predict the hydrogen bond network of the 3-oxo-12α-hydroxy derivative [8]. On the other hand, the ability to form hydrogen bonds by CA plus the characteristics of head-to-head dimers have been used for designing a crystal, in which a single water molecule is encapsulated between two cholic residues in an ice-like structure [17]. Miyata et al. have also studied the supramolecular chirality in crystals generated from chiral [37–40] and achiral [41,42] molecules, and rationalized a hierarchical organization in BA crystals like that in proteins [3,43,44].

Nowadays interesting and promising applications have emerged, mainly related to the ability of BA to form inclusion compounds in the solid state. For example, the crystallization may be used for the resolution of racemates [13,45–50] and for the delayed release of drugs [32].

Although BS have been the object of numerous studies by different techniques concerning to their surfactant behavior in solution, the number of publications related to their crystal structures is limited, and much lower than those corresponding to BA and BE. Some structures of the derivatives outlined before in the solid state have also been reported, including some dimers. In the case of head-to-head dimers, an internal coordinate system consisting of five angles (three torsion and two common) has been proposed [51] to describe the relative orientation in the space of the two bile acid residues.

When analyzing the structure of steroid derivatives, most of the studies have mainly focused the attention on the flexibility of the side chain and on the hydrogen bond network, while the structure of the steroid nucleus is barely mentioned, with the exception of the D-ring conformation. Only some recent papers have introduced the analysis of the angle formed by horizontal and vertical planes [10] and the angle between C3-C10-C13 carbon atoms [51]. The comparison of structural data from published crystal structures of bile acid derivatives will provide information on the constancy (or lack thereof) of the geometrical parameters of the steroid nucleus. It will also allow for obtaining the average geometrical parameters of the steroid nucleus. Thus, average distances and bond angles of the cyclopentanoperhydrophenanthrene skeleton and the lateral chain can be obtained. This average structure can be useful as a standard reference for further comparative studies. For example, it will allow for the analysis of the resulting geometry when important chemical modifications are introduced to the structure.

In this paper, we analyze the crystal structures of two BEs derived from CA: a dimer with the two steroid units linked by a urea bridge (**30**, Table 2), and a monomer with an amino isophthalic residue attached to the C3 position of the steroid nucleus (**24**, Table 1). The geometric characteristics of these two BEs, together with those corresponding to 28 other structures (mainly from CA and DCA solved by our research group, Tables 1 and 2), are used to construct the standard steroid.

Table 2. Chemical structure and partial numbering of the dimers analyzed in this paper (**30**/AcOEt and **30**/DMSO make reference to the recrystallization solvent included as a guest in the crystal structure).

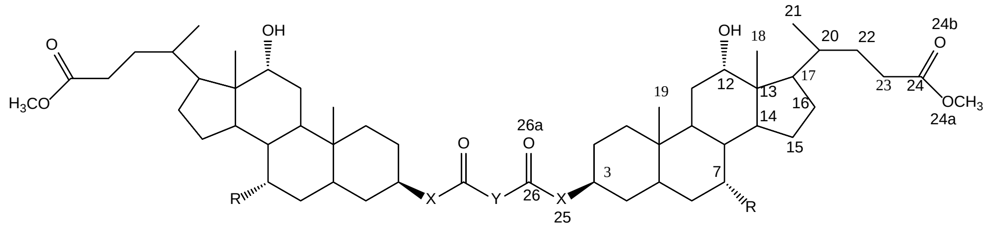

R	X	Y	Compound	Reference
α-OH	β-NH	$-CH_2CH_2-$	**27**	[17]
α-OH	β-NH	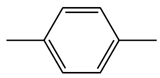	**28**	[51]
H	α-O	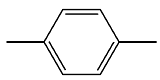	**29**	[51]
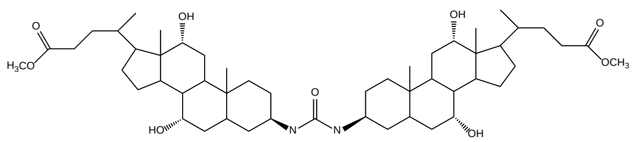			**30**/AcOEt **30**/DMSO	this paper [52]

2. Materials and Methods

2.1. Synthesis

To synthesize compound **24**, 0.77 mL (4.55 mmol) of DEPC were added to a dispersion of 2 g (4.75 mmol) of methyl 3β-aminocholate (the synthesis of this reactive has been well-established [53]), in 15 mL of dimethylformamide under an argon atmosphere. Once the solid was dissolved, 2.32 g (5.5 mmol) of 5-*t*-butoxycarbonylaminoisophthalic acid was added, and the mixture was stirred for 10 min (the protection of the amino group of the amino isophthalic acid with di-*tert*-butyl dicarbonate (BOC) is also a well-known synthetic process [54]. After cooling at 0 °C, 1 mL (7 mmol) of triethylamine was added dropwise. The reaction mixture was maintained at this temperature for 45 min, and then at room temperature for 6 h. DMF was evaporated under reduced pressure; the reaction crude dissolved in 200 mL of ethyl acetate and was washed with 3 × 75 mL of water. The organic phase was dried with sodium sulphate, concentrated, and purified by column chromatography with 20:1 ethyl acetate:methanol. Finally, BOC was removed, dissolving 2 g of the product obtained in the last step in 50 mL of methanol and bubbling HCl gas for 30 min. After evaporation of the solvent, 100 mL of water was added, and the solution was neutralized with 1 M NaOH until neutral pH in an ice bath. The solid corresponding to compound **24** was filtered, washed with abundant water, and dried in a vacuum oven. Its characterization was done by X-ray diffraction.

The synthesis of the dimer listed as compound **30** has been reported previously [51].

2.2. X-ray Diffraction Analysis

Colorless prismatic crystals of compound **24** were obtained from methanol, and crystals of compound **30** in ethyl acetate/methanol. X-ray diffraction data for both compounds were collected on a Bruker Smart-CCD-1000 at the temperature of 100 K. Molecular graphics were made with Mercury software. CIF files are available as electronic supporting material. CCDC 1812924 and 1812925 contain the supplementary crystallographic data for compounds **24** and **30**, respectively, and can be obtained free of charge from The Cambridge Crystallographic Data Center.

3. Results and Discussion

3.1. Dimer

The crystal structure of compound **30** from DMSO/methanol has been obtained and published [52] (we will refer to it as **30**/DMSO). In this paper, we instead describe the crystal obtained from ethyl acetate/methanol (**30**/AcOEt). Table 3 shows a summary of the crystal data and experimental details. The dimer crystallized in the $P2_12_12_1$ space group, and its packing showed a bilayer structure, with alternating hydrophobic and hydrophilic layers. The horizontal planes [10] of the two cholic residues were almost parallel (0.92° being the angle between them), meaning that their α-faces are oriented to the same direction, transmitting the bifacial character of each steroid residue to the dimer. Within the layers, dimers are located in a face-to-face orientation, with β-interdigitation between C18 and C19 methyl groups (Figure 1a), contributing to the stabilization of the bilayer by hydrophobic forces (a similar situation appears in **30**/DMSO, Figure 1b).

Table 3. Crystal data, data collection, and refinement for **30** recrystallized from AcOEt/MeOH and **24** recrystallized from MeOH.

Compound	30/AcOEt	24
Empirical formula	$C_{51}H_{84}N_2O_9$,$C_4H_8O_2$,2(CH_4O), H_2O	$C_{34}H_{50}N_2O_7$, H_2O
Formula weight	1039.40	616.78
Temperature (K)	100(2)	100(2)
Wavelength (Å)	0.71073	0.71073
Crystal system, space group	Orthorhombic, $P2_12_12_1$	Monoclinic, $P2_1$
a (Å)	7.5548(2)	13.608(3)
b (Å)	15.2458(5)	7.704(10)
c (Å)	49.3048(15)	30.284(5)
α (°)	90	90
β (°)	90	96.345(10)
γ (°)	90	90
Volume ($Å^3$)	5678.9(3)	3155.68(10)
Z, calculated density (g/cm^3)	4, 1.216	4, 1.298
Absorption coefficient (mm^{-1})	0.085	0.092
F (000)	2280	1336
Crystal size (mm^3)	0.400 × 0.160 × 0.050	0.21 × 0.10 × 0.05
Theta range (data collection) (°)	1.570 to 26.412	1.35 to 26.81
Index ranges	$-9 \leq h \leq 9, -18 \leq k \leq 19, -61 \leq l \leq 52$	$-17 \leq h \leq 17, -9 \leq k \leq 9, -38 \leq l \leq 38$
Data/restraints/parameters	11,614/112/703	7250/3/845
Goodnes-of fit on F^2	1.022	1.011
Final R indices [I > 2σ(I)	R1 = 0.0746, wR2 = 0.1643	R1 = 0.0518, wR2 = 0.0.978
R indices (all data)	R1 = 0.1382, wR2 = 0.1946	R1 = 0.1016, wR2 = 0.1157

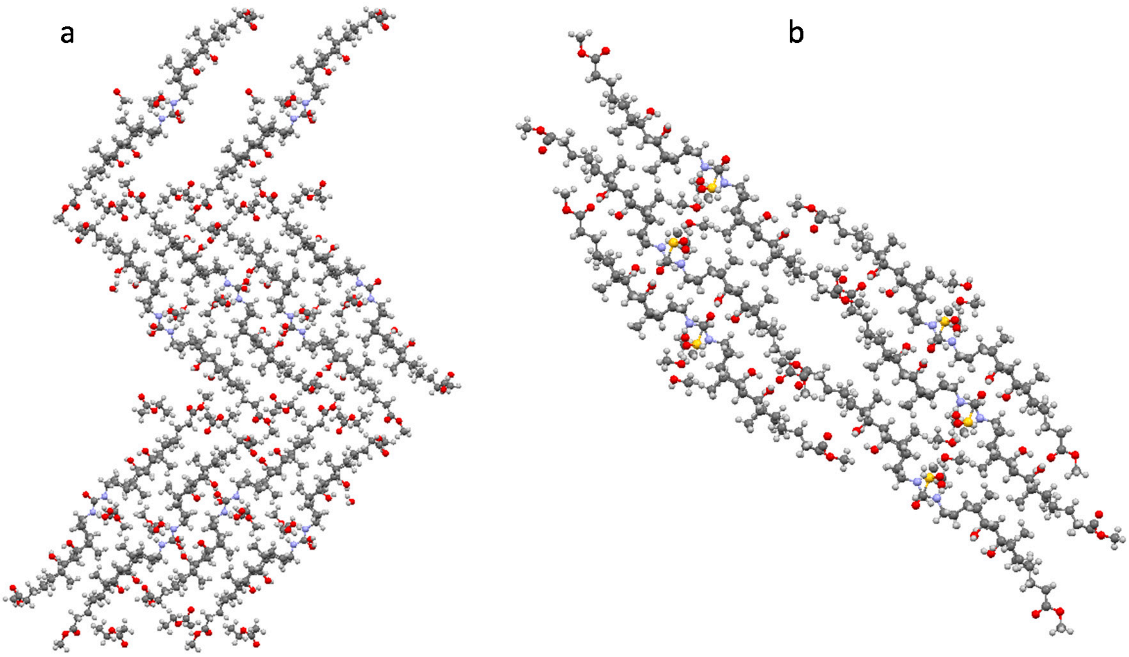

Figure 1. View of the molecular packing along the *a* axis (**a**) in the crystal of **30**/AcOEt and (**b**) along the *b* axis in the crystal of **30**/DMSO.

Additional stabilization arises from the hydrogen bonding network, involving the nitrogen and oxygen atoms of the urea bridge (all O7H and O12H groups), and one of the two carboxylic terminal groups of the dimer. The hydrogen bonding pattern in the constituent monomer, with the free carboxylic group (without hydrogen bonds), is the same as in **30**/DMSO. The lateral chains adopt a *tttt* conformation in both cases. In the other monomer, the hydrogen bond pattern is the same as in **30**/DMSO, except for an additional bond between O7H and water (Figure 2). This difference could explain why this monomer in **30**/AcOEt adopts a $ttgi_{tg}$ conformation while in **30**/DMSO it also adopts a *tttt* one. The angle between horizontal planes is higher in **30**/DMSO (4.9°), and the angles between vertical planes are 1.2° and 8.7° in **30**/DMSO and **30**/AcOEt, respectively.

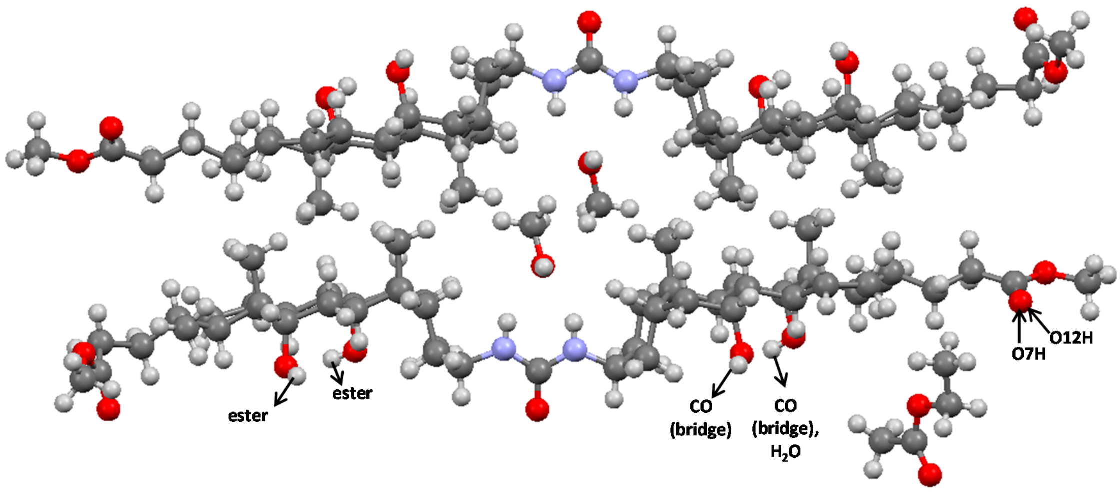

Figure 2. Scheme of the hydrogen bonds involving the two monomers in the dimer 30/AcOEt.

On the other hand, the monomers in the dimer are placed in such a way that the resulting values for the common angles, θ_i, and the torsion (or dihedral) angles, φ_i, are θ_1 = 123.1°, θ_2 = 129.5°,

$\varphi_1 = 4.7°$, $\varphi_2 = 174.3°$ and $\varphi_3 = -175.4°$. Therefore, the dimer crystallizes as a *tet* (*anti-eclipsed-anti*) conformer (Figure 3), the same as in **30**/DMSO.

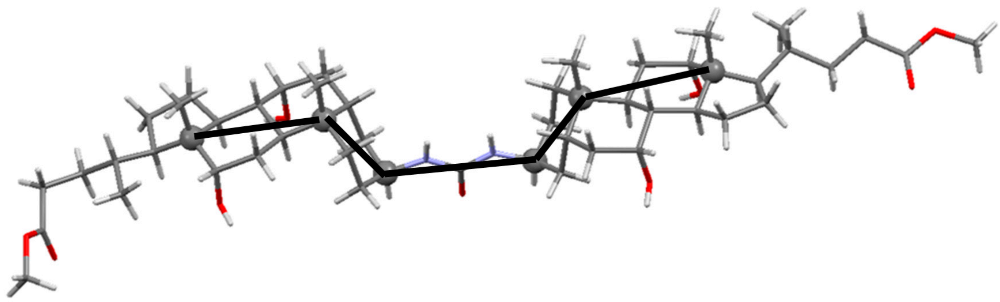

Figure 3. Perspective view of the conformer in the crystal structure of 30/AcOEt, showing its *tet* conformation.

Although many analogies have been found between **30**/DMSO and **30**/AcOEt, the main difference between the two crystal structures concerns the constitution of the bilayers. Although the bilayers in both structures have similar widths (11.36 Å in **30**/DMSO and 10.98 Å in **30**/AcOEt), they are linear in **30**/DMSO and corrugated in **30**/AcOEt (Figure 1). The result is that the crystals belong to different space groups, being monoclinic I2 for **30**/DMSO. This agrees with the well-known fact that the solvent can modify the final crystal structure of bile acids and derivatives [14,55,56].

Table 4 shows details of the crystal structures for these and other different BE dimers. As a brief summary of the conclusions deduced by comparison of the results we can mention: (1) Four of the five dimers crystallize in the monoclinic crystal system, three of them in the $P2_1$ and the other in the I2. In this case, corresponding to **30**/DMSO, apart from the screw axis typical of the $P2_1$ crystals, the crystal structure also presents a centring vector [1/2,1/2,1/2] and a 2-fold rotation axis with direction [0,1,0] at 0,y,0. The crystal corresponding to the remaining dimer, **30**/AcOEt, is orthorhombic $P2_12_12_1$. (2) The *tet* conformation is the most common one. (3) All these dimers have the tendency to be arranged with the lateral chains fully or nearly fully extended. (4) With the exception of **28**, in the crystal structures of the other three dimers where the molecules are arranged in bilayers, these are β interdigitated. The bilayers are corrugated in **30**/AcOEt and **28** and linear in **30**/DMSO and **27**. The thicknesses of the corrugated bilayers are slightly smaller than the thicknesses of the linear bilayers (Table 4).

Table 4. Some characteristics of the crystal structures of the BE dimers analyzed in this paper.

Dimer	Space Group	Conformer	Lateral Chain Conformation	Type of Bilayer/Width (Å)	Interdigitation	Ref.
30/AcOEt	$P2_12_12_1$	*tet*	*tttt/ttgi*$_{tg}$	corrugated/10.98	β	this work
30/DMSO	I2	*tet*	*tttt/tttt*	linear/11.36	β	[52]
28	$P2_1$	*tet*	*tttt/tgtt*	corrugated/10.98	-	[51]
27	$P2_1$	*ttt*	*tttg/tttt*	linear/11.30	β	[51]
29	$P2_1$	$i_{eg}ti_{eg}$	*ttti/ttgc*	-	-	[51]

3.2. Monomer

A summary of the crystal data and experimental details corresponding to this diester derivative of CA (with a 5-amino-isophthalic group attached to the 3β position of the steroid nucleus, through an amide bond in compound **24**) is listed in Table 3. This dimer crystallizes in the monoclinic $P2_1$ space group with one guest water molecule, having the asymmetric unit formed by two different molecules of the steroid. The main difference between these two molecules concerns the conformation of the D ring, since the phase angle of pseudorotation values [57] are indicatives of half chair and close to β-envelope conformations. However, the conformations of the lateral chains are very similar, both being *tgtt*.

Figure 4 presents the view of packing in the crystal along the *b* axis, and shows a bilayer organization of α interdigitated molecules, with a width of 13.54 Å. This bilayer is stabilized by hydrogen bonds between molecules of the same geometry (identical color in Figure 4), as well as by a π-π stacking between the aromatic rings of two molecules with different geometry (different color in Figure 4). The aromatic planes are almost parallel (with an angle of 1.97°), the benzyl rings being slightly displaced. The distance between their centroids is 3.349 Å (Figure 5) and the distance of the centroid-aromatic plane is 3.193 Å. These values are similar to those published for other aromatic compounds [58], including graphite [59]. On the other hand, the limit to the π-π interaction is the summation of the van der Waals radii between the involved atoms. Alvarez [60] has suggested that an accurate van der Waals radius for the carbon atom is equal to 1.77 Å. Therefore, the maximum distance for a π-π interaction would be 3.54 Å, a value which agrees well with the one given above.

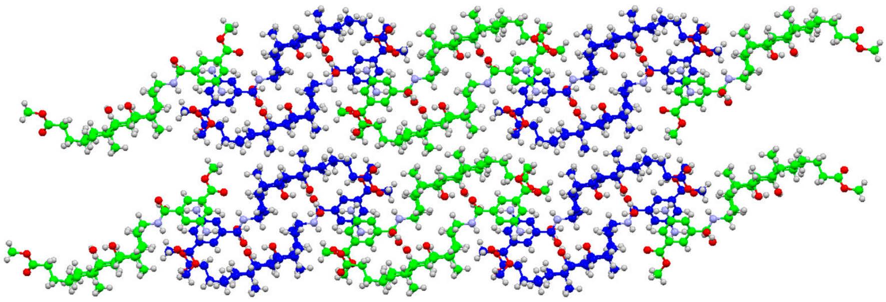

Figure 4. View of crystal packing of compound **24** along the *b* axis. For clarity, the carbon atoms of the two molecules of the asymmetric unit are drawn in different colors.

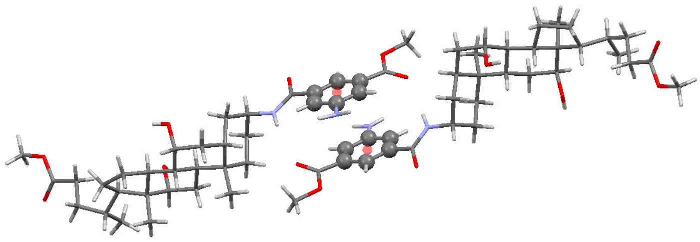

Figure 5. View of the crystal packing of compound **24** along a direction in which the π-π interaction is clearly seen. The red points correspond to the centroids of the involved aromatic rings.

It is remarkable that only molecules with different symmetry are linked through hydrogen bonds, the pattern being the same for both molecules. The interaction implies the amide C=O, O7H and O12H groups. This last group acts as an acceptor from water hosted at the hydrophilic part of the bilayer. Neither the ester at the lateral chain, nor the amine group in the aromatic substituent participates in the hydrogen bonding network in the crystal.

3.3. Standard Steroid

We have analyzed the structures of the steroid moiety of all the compounds listed in Tables 1 and 2, paying attention to the bond distances and bond angles between carbon atoms. Some compounds were recrystallized from several solvents (resulting in their inclusion as guests), while others crystallized with two different molecules in the asymmetric unit. The total number of data is 48.

Table 5 shows the values of the mean distances between bonded carbon atoms in the steroid skeleton, including the 18 and 19 methyl groups and the atoms of the lateral chain. The shortest and largest lengths are 1.502 ± 0.020 Å and 1.558 ± 0.010 Å, corresponding to C23-C24 and C9-C10 bonds, respectively. As expected, the differences in the distances among the different compounds analyzed are small, particularly in the more condensed B and C rings. Figure 6a analyzes those results according to the standard deviations in the bond lengths, which are less than 0.01 Å (those in green), between 0.01 and 0.015 Å (those in black), and greater than 0.015 Å (those in red). In a similar way, we have determined the mean values of all the angles between consecutive carbon atoms in the steroid nucleus and the lateral chain, the results being recompiled in Table 6 (the angle C2-C3-C4 was not considered for **11** because of the sp^2 hybridization of the central atom). The highest value corresponds to the C13-C17-C20 angle (119.4°), and the lowest to C17-C13-C14 (100.2°) inside the cyclopentane ring. The angle C17-C20-C22 (in the flexible lateral chain) shows the highest standard deviation, and surprisingly, the angle C9-C10-C19 presents the highest constancy of values for the compounds analyzed. The results were also analyzed according to their standard deviations in Figure 6b (color code: ≤0.75° green, 0.75–1.50° black, and >1.50° red).

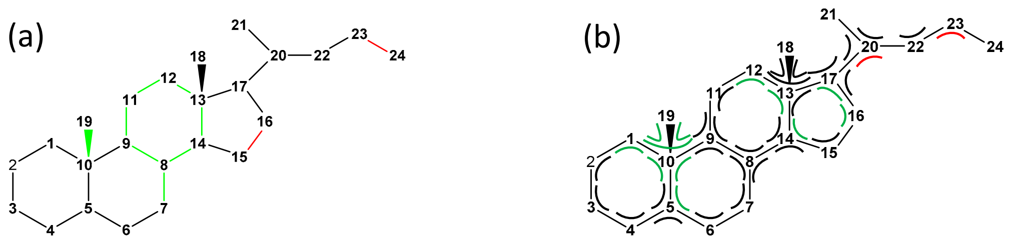

Figure 6. Standard steroid according to (**a**) the bond lengths and (**b**) bond angles and their respective standard deviations (see text).

Table 5. Mean distances and standard deviations for the bond lengths of the steroids analyzed in this paper, and comparison with progesterone and the lateral chain of cholesterol.

Standard Steroid		**Progesterone**	**Cholesterol**
bond	mean distance ± standard deviation (Å)	distance/difference (Å)	mean distance/difference (Å)
C1-C2	1.522 ± 0.012	1.533/−0.011	
C2-C3	1.519 ± 0.011	1.498/0.021	
C3-C4	1.521 ± 0.012	1.466/0.055	
C4-C5	1.537 ± 0.011	1.347/0.190	
C5-C10	1.548 ± 0.014	1.527/0.021	
C10-C1	1.540 ± 0.011	1.539/0.001	
C5-C6	1.534 ± 0.011	1.504/0.030	
C6-C7	1.526 ± 0.013	1.521/0.005	
C7-C8	1.528 ± 0.009	1.529/-0.001	
C8-C9	1.544 ± 0.009	1.538/0.00613	
C9-C10	1.558 ± 0.010	1.502/0.05614	
C10-C19	1.538 ± 0.010	1.544/−0.006	
C9-C11	1.537 ± 0.009	1.535/0.002	
C11-C12	1.531 ± 0.008	1.546/−0.015	
C12-C13	1.535 ± 0.009	1.535/0.000	
C13-C14	1.543 ± 0.010	1.547/−0.004	
C14-C8	1.523 ± 0.007	1.524/−0.001	
C13-C18	1.535 ± 0.011	1.538/−0.003	
C14-C15	1.529 ± 0.012	1.538/−0.009	
C15-C16	1.541 ± 0.021	1.543/−0.002	
C16-C17	1.556 ± 0.011	1.549/0.007	
C17-C13	1.554 ± 0.011	1.564/−0.010	
C17-C20	1.539 ± 0.010		1.544/−0.005
C20-C21	1.527 ± 0.011		1.527/0.00
C20-C22	1.540 ± 0.012		1.535/0.005
C22-C23	1.523 ± 0.014		1.516/0.007
C23-C24	1.502 ± 0.020		1.569/−0.067

Table 6. Mean values and standard deviations for the bond angles of the steroids analyzed in this paper, and comparison with progesterone and the lateral chain of cholesterol.

Standard Steroid		**Progesterone**	**Cholesterol**
angle	mean value ± standard deviation (°)	angle/difference (°)	mean angle/ difference (°)
C10-C1-C2	114.6 ± 0.6	114.4/0.2	
C1-C2-C3	110.8 ± 1.1	111.7/−0.9	
C2-C3-C4	110.5 ± 0.9	117.0/−6.5	
C3-C4-C5	113.7 ± 1.4	123.7/−10.0	
C4-C5-C10	113.1 ± 0.8	123.0/−9.9	
C5-C10-C1	108.0 ± 0.7	109.4/−1.4	
C4-C5-C6	111.1 ± 0.9	119.8/−8.7	
C5-C6-C7	114.0 ± 1.3	112.0/2.0	
C6-C7-C8	111.9 ± 1.4	111.9/0.0	
C7-C8-C9	111.1 ± 1.3	110.8/0.4	
C8-C9-C10	111.7 ± 0.9	114.8/−3.1	
C9-C10-C1	112.4 ± 0.8	108.5/3.9	
C9-C10-C5	108.8 ± 0.6	109.5/−0.7	
C10-C5-C6	111.9 ± 0.5	117.3/−5.4	
C1-C10-C19	106.5 ± 0.7	110.2/−3.7	
C5-C10-C19	109.7 ± 0.7	107.3/2.4	
C9-C10-C19	111.5 ± 0.5	111.9/−0.4	
C7-C8-C14	112.1 ± 0.9	111.3/0.8	
C8-C14-C13	114.5 ± 1.1	114.1/0.4	
C14-C13-C12	107.3 ± 0.8	107.6/−0.3	
C13-C12-C11	111.2 ± 0.7	111.2/0.0	
C12-C11-C9	114.4 ± 1.2	112.9/1.5	
C11-C9-C10	113.6 ± 0.9	112.8/0.8	
C11-C9-C8	111.6 ± 1.2	111.1/0.5	
C9-C8-C14	109.7 ± 1.3	107.9/1.8	
C8-C14-C15	118.3 ± 1.0	120.2/−1.9	
C14-C15-C16	103.9 ± 0.8	103.9/−0.0	
C15-C16-C17	107.0 ± 0.7	106.6/0.6	
C16-C17-C13	103.1 ± 0.7	104.7/−1.6	
C17-C13-C14	100.2 ± 0.8	99.7/0.5	
C17-C13-C12	117.1 ± 1.1	116.0/1.1	
C13-C14-C15	103.9 ± 0.5	103.5/0.4	
C12-C13-C18	109.4 ± 1.0	111.2/−1.8	
C14-C13-C18	112.6 ± 0.6	112.4/0.2	
C17-C13-C18	110.0 ± 0.9	109.5/0.5	
C16-C17-C20	112.3 ± 1.0	114.0/−1.7	111.2/1.1
C13-C17-C20	119.4 ± 1.1	115.9/3.5	120.0/−0.6
C17-C20-C21	112.9 ± 1.1		112.0/0.9
C17-C20-C22	110.3 ± 2.0		110.0/0.3
C21-C20-C22	110.3 ± 0.9		110.5/−0.2
C20-C22-C23	114.5 ± 1.3		115.0/−0.5
C22-C23-C24	113.7 ± 1.7		111.5/2.2

Tables 5 and 6 and Figure 6 define the average steroid nucleus. We can now analyze how this model steroid changes because of significant modifications in the steroid structure.

As examples, we have chosen progesterone (Figure 7a) to analyze the cyclopentanoperhydrophenanthrene nucleus, and cholesterol (Figure 7b) for the lateral chain analysis. Data were obtained from the CIF files reported by Shikii et al. for progesterone [61], and Shieh et al. for cholesterol [62]. Since the asymmetric unit in the crystal of cholesterol has eight molecules, mean values of bond distances and bond angles were calculated for comparison purposes.

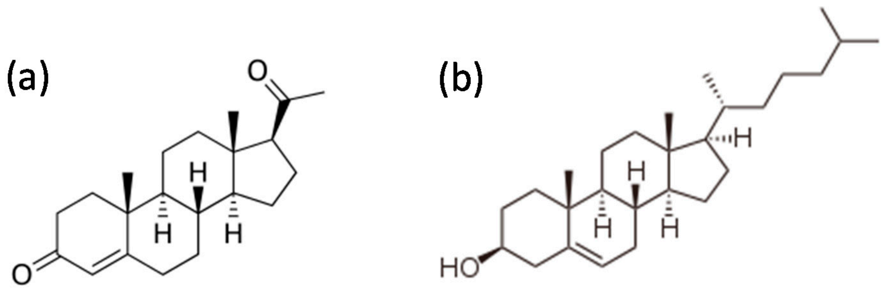

Figure 7. Chemical structures of (**a**) progesterone and (**b**) cholesterol.

In progesterone, apart from the length corresponding to the C4-C5 double bond, the other lengths presenting differences with the standard steroid (greater than 0.015 Å) are those corresponding to the C4-C5 bond's neighbors (C3-C4 and C5-C10), as well as the C2-C3, C5-C6 and C9-C10 bonds. Excluding the bond angles in which C2, C3, and C4 atoms (participating in double bonds) are involved, the remaining values do not differ greatly from those of the standard steroid. In fact, the differences between them are similar to those observed between the compounds used to define the standard steroid.

In cholesterol, only the C23-C24 bond length is greater than 0.015 Å in comparison to this length in the standard steroid. On the other hand, the differences between the bond angles are very small, the greatest being 2.2° in the C22-C23-C24 bond angle.

Although significant changes are not to be expected, we have also calculated the angles between the horizontal and vertical planes for the steroid molecules in the 48 structures resulting in the crystal packings. The results are shown in Table 7, and the main conclusion is the confirmation of the validity of these two planes for comparisons and discussions. The average angle value for the standard steroid is 88.2 ± 0.5°. Therefore, the standard steroid defined here behaves very well in the discussed aspects.

Table 7. Values of the angles between the horizontal and vertical planes, and conformations of the lateral chain in the steroids analyzed in this paper (a and b refer either to the two molecules in the asymmetric unit, or to the two monomers in a dimer).

Compound	Angle Between Horizontal and Vertical Planes (°)	Lateral Chain Conformation
1	88.2	*tttg*
2	88.4	*tgtt*
3a	87.9	*tgti*$_{tg}$
3b	88.3	*tgti*$_{tg}$
4	87.6	*gtgc*
5	88.0	*gttt*
6	87.2	*tttc*
7	88.0	*ttgg*
8a	89.4	*ttti*$_{tg}$
8b	87.9	*tgtg*
9	87.9	*tttg*
10	88.7	*tttt*
11a	89.0	*tgtt*
11b	89.8	*tgtt*
12	88.9	*ttt-*
13	88.0	*tgtt*
14	88.0	*tgtt*
15/2-propanol	88.4	*tgtg*
15/acetone	87.7	*ttti*$_{tg}$
15/DMSO	87.9	*tttt*
16/acetone a	87.5	*ttgt*
16/acetone b	87.3	*ttgt*
16/chlorobenzene	87.9	*ttgt*

Table 7. *Cont.*

Compound	Angle Between Horizontal and Vertical Planes (°)	Lateral Chain Conformation
17	87.8	*tttt*
18	88.4	*ttgi*$_{tg}$
19	88.0	*ttgi*$_{tg}$
20	88.3	*tttt*
21a	88.7	*tttt*
21b	88.4	*tttt*
22a	88.7	*tttt*
22b	88.7	*ttgt*
23	88.1	*tttc*
24a	88.1	*tgtt*
24b	87.8	*tgtt*
25/DMSO	88.8	*ttgi*$_{tg}$
25/MeOH	87.9	*ttgg*
25/acetone	87.7	*ttgg*
26	87.9	*ttgt*
27a	88.6	*tttg*
27b	88.6	*tttt*
28a	87.9	*tgtt*
28b	88.4	*tttt*
29a	86.8	*ttti*$_{tg}$
29b	87.9	*ttgc*
30/AcOEt a	87.9	*tttt*
30/AcOEt b	88.2	*ttgi*$_{tg}$
30/DMSO a	88.4	*tttt*
30/DMSO b	88.6	*tttt*

The analysis of the conformation of the lateral chain can be made through the positions of its atoms with respect to the horizontal and vertical planes (for example), or through the torsion angles from C17 to C23. However, the geometric requirements needed for the establishment of hydrogen bonds a priori indicate that the result can be very variable (see above). Therefore, for discussing the lateral chains, the second option is more appropriate. Results are recompiled in Table 7. With the exceptions of derivatives, compounds **4** and **5** (for which it is *gauche*), the other 46 crystal structures have *trans* conformations in the C13-C17-C20-C22 torsion angle. This predominant conformation is a consequence of the torsion angle C13-C17-C20-C21, which, being in the narrow range −53/−60°, corresponds to a minimum in the energy profile for cholanic acids and related compounds [63]. This minimum is also associated with values of about 60 and −170° for C17-C20-C22-C23 (the second torsion angle), corresponding to *gauche* and *trans* conformations, respectively. Of the found conformations, 75% are *trans*, and the remaining are *gauche*. The mentioned minimum has also values around 50 (*gauche*), 165 (*trans*), and −95° (intermediate between *gauche* and *trans*, i_{tg}) for C20-C22-C23-C24. For this third torsion angle, the *trans* conformation appears in 71% of the crystal structures, while 29% are *gauche*. Finally, the conformations found for the torsion angle C22-C23-C24-O24a are the following: *trans* 55.5%, i_{tg} 19%, *gauche* 17%, and *cis* 8.5%. Therefore, the variability in the conformations is greater when we move to the end of the lateral change (although *trans* conformations are the most common ones). This fact is a consequence of the fact that the atoms of the carboxylic group adopt positions controlled by the formation of hydrogen bonds (favored by the flexibility of the lateral chain in cholanic acids), and such a conformation is not characteristic of a specific BA and their derivatives. Indeed, the *cis* conformation appears in two epimers of DCA (compounds **4** and **6**), the azide derivative of CA compound **23**, and one of the molecules of the dimer compound **29** (the one in which its lateral chain does not participate in hydrogen bonding).

Finally, we have recompiled some information about the hydrogen bonding network in the crystal structures of monomers. We have considered the compounds with hydroxy, oxo, or amide groups at the C3 position, and hydroxy groups at the C7 or C12 positions, i.e., all the compounds of Table 3 excluding the amine (compounds **12**, **21** and **22**), azide (compound **23**) and ester (compound **26**) derivatives. The participation of water as a guest was also considered, but not other solvents. Table 8 shows the mean distances of the donor-H/acceptor systems determined from the analysis of the structures, where the donor/acceptor behavior is not specified. In the Table, values without standard deviations were found in only one crystal.

Table 8. Mean values with standard deviations for the donor/acceptor distance in the indicated hydrogen bonds of the monomers indicated in the text. Units of all data in Å.

	O7H	**O12H**	**O24b=COR**	**OC-O24a-R**	**CO-(NH)**	**(CO)-NH**	**Water**
O3H	2.75 ± 0.11	2.720 ± 0.05	2.76 ± 0.08	2.64 ± 0.04			
O7H	2.803	2.793	2.851 ± 0.016	2.640 ± 0.015	2.78 ± 0.10		2.79 ± 0.09
O12H			2.88 ± 0.04	2.680 ± 0.030	2.81 ± 0.07		2.86 ± 0.10
O24b=COR				2.803		3.008 ± 0.019	2.75 ± 0.11
OC-O24a-R					2.588	2.978	2.579 ± 0.021

It may be noticed that O3H can form hydrogen bonds with any of the hydrophylic groups present in the steroids, with the exception of the amide group (when present) and itself. This last observation also applies to O12H, but not to O7H. In only one structure, compound **8**, the carboxylic groups directly formed a hydrogen bond. All the values are within accepted ones for hydrogen bonds.

In cholesterol, which only has one hydroxy group at C3, only a O3/O3 hydrogen bond is possible. The average bond length for that bond is 2.87 ± 0.07 Å. In the absence of an appropriate solvent, progesterone cannot form any hydrogen bond.

Supplementary Materials: The following are available online at http://www.mdpi.com/2073-4352/8/2/86/s1.

Acknowledgments: The authors thank the Ministerio de Ciencia y Tecnología (Project MAT2013-45657-P) for financial support.

Author Contributions: F.M. and J.V.T. conceived and designed the experiments; S.d.F., V.H.S., J.A.S. and M.P.V-T performed the synthesis and the recrystallization of compounds; A.J., J.A.S. and F.F. analyzed the data; F.M. and S.d.F. collected data from crystal structures and performed calculations; F.M. and J.V.T. wrote the paper.

Conflicts of Interest: The authors declare no conflicts of interest.

References

1. Enhsen, A.; Kramer, W.; Wess, G. Bile acids in drug discovery. *Drug Discov. Today* **1998**, *3*, 409–418. [CrossRef]
2. Hofmann, A.F.; Hagey, L.R. Key discoveries in bile acid chemistry and biology and their clinical applications: History of the last eight decades. *J. Lipid Res.* **2014**, *55*, 1553–1595. [CrossRef] [PubMed]
3. Miyata, M.; Tohnai, N.; Hisaki, I. Crystalline Host-Guest Assemblies of Steroidal and Related Molecules: Diversity, Hierarchy, and Supramolecular Chirality. *Acc. Chem. Res.* **2007**, *40*, 694–702. [CrossRef] [PubMed]
4. Coello, A.; Meijide, F.; Rodríguez Núñez, E.; Vázquez Tato, J. Aggregation Behavior of Bile Salts in Aqueous Solution. *J. Pharm. Sci.* **1996**, *85*, 9–15. [CrossRef] [PubMed]
5. Madenci, D.; Egelhaaf, S.U. Self-assembly in aqueous bile salt solutions. *Curr. Opin. Colloid Interface Sci.* **2010**, *15*, 109–115. [CrossRef]
6. Miki, K.; Kasai, N.; Shibakami, M.; Chirachanchai, S.; Takemoto, K.; Miyata, M. Crystal structure of cholic acid with no guest molecules. *Acta Cryst. C* **1990**, *46*, 2442–2445. [CrossRef]
7. Arora, S.K.; Germain, G.; Declercq, J.P. The crystal and molecular structure of lithocholic acid. *Acta Cryst. B* **1976**, *32*, 415–419. [CrossRef]
8. Jover, A.; Meijide, F.; Soto, V.H.; Vázquez Tato, J.; Rodríguez Núñez, E.; Ton-Nu, H.-T.; Hofmann, A.F. Successful prediction of the hydrogen bond network of the 3-oxo-12α-hydroxy-5β-cholan-24-oic acid crystal from resolution of the crystal structure of deoxycholic acid and its three 3,12-dihydroxy epimers. *Steroids* **2004**, *69*, 379–388. [CrossRef] [PubMed]
9. Jover, A.; Meijide, F.; Rodríguez Núñez, E.; Vázquez Tato, J.; Castiñeiras, A.; Hofmann, A.F.; Ton-nu, H.-T. Crystal structure of 3β,12α-dihydroxy-5β-cholan-24-oic acid (iso-deoxycholic acid). *J. Mol. Struct.* **2000**, *523*, 299–307. [CrossRef]

10. Alvarez, M.; Jover, A.; Carrazana, J.; Meijide, F.; Soto, V.H.; Vázquez Tato, J. Crystal structure of chenodeoxycholic acid, ursodeoxycholic acid and their two 3β,7α- and 3β,7β-dihydroxy epimers. *Steroids* **2007**, *72*, 535–544. [CrossRef] [PubMed]
11. Meijide, F.; Antelo, A.; Alvarez, M.; Soto, V.H.; Trillo, J.V.; Jover, A.; Vázquez Tato, J. Spontaneous formation in solid state of carbamate derivatives of bile acids. *Cryst. Growth Des.* **2011**, *11*, 356–361. [CrossRef]
12. Soto, V.H.; Jover, A.; Galantini, L.; Pavel, N.V.; Meijide, F.; Vázquez Tato, J. New Lamellar Structure Formed by an Adamantyl Derivative of Cholic Acid. *J. Phys. Chem. B* **2006**, *110*, 13679–13681. [CrossRef] [PubMed]
13. Miragaya, J.; Jover, A.; Fraga, F.; Meijide, F.; Vázquez Tato, J. Enantioresolution and Chameleonic Mimicry of 2-Butanol with an Adamantylacetyl Derivative of Cholic Acid. *Crystal Growth Des.* **2010**, *10*, 1124–1129. [CrossRef]
14. Miragaya, J.; Jover, A.; Fraga, F.; Meijide, F.; Vázquez Tato, J. Influence of the solvent ability to form hydrogen bonds in the crystal structure of ([3β,5β,7α,12α]-3[(norbornyl-2-acetyl)-amino]-7,12-dihydroxycholan-24-oic acid (a norbornyl derivative of cholic acid). *Steroids* **2009**, *74*, 735–741. [CrossRef] [PubMed]
15. Meijide, F.; Trillo, J.V.; Soto, V.H.; Jover, A.; Vázquez Tato, J. Additional criterion for the determination of the handedness of 21 helices in crystals of bile acids: Crystal structure of a tert-butylphenyl derivative of cholic acid. *Chirality* **2011**, *23*, 940–947. [CrossRef] [PubMed]
16. Meijide, F.; Trillo, J.V.; de Frutos, S.; Galantini, L.; Pavel, N.V.; Soto, V.H.; Jover, A.; Vázquez Tato, J. Formation of tubules by p-tert-butylphenylamide derivatives of chenodeoxycholic and ursodeoxycholic acids in aqueous solution. *Steroids* **2012**, *77*, 1205–1211. [CrossRef] [PubMed]
17. Soto, V.H.; Alvarez, M.; Meijide, F.; Trillo, J.V.; Antelo, A.; Jover, A.; Galantini, L.; Vázquez Tato, J. Ice-like encapsulated water by two cholic acid moieties. *Steroids* **2012**, *77*, 1228–1232. [CrossRef] [PubMed]
18. Galantini, L.; di Gregorio, M.C.; Gubitosi, M.; Travaglini, L.; Vázquez Tato, J.; Jover, A.; Meijide, F.; Soto, V.H.; Pavel, N.V. Bile salts and derivatives: Rigid unconventional amphiphiles as dispersants, carriers and superstructure building blocks. *Curr. Opin. Colloid Interface Sci.* **2015**, *20*, 170–182. [CrossRef]
19. Yoshii, M.; Yamamura, M.; Satake, A.; Kobuke, Y. Supramolecular ion channels from a transmembrane bischolic acid derivative showing two discrete conductances. *Org. Biomol. Chem.* **2004**, *2*, 2619–2623. [CrossRef] [PubMed]
20. Wess, G.; Kramer, W.; Enhsen, A.; Glombik, H.; Baringhaus, K.-H.; Boeger, G.; Urmann, M.; Bock, K.; Kleine, H.; Neckermann, G.; et al. Specific Inhibitors of Ileal Bile Acid Transport. *J. Med. Chem.* **1994**, *37*, 873–875. [CrossRef] [PubMed]
21. Alvarez, M.; Jover, A.; Meijide, F.; Galantini, L.; Pavel, N.V.; Antelo, A.; Vázquez Tato, J. Synthesis and Characterization of a New Gemini Surfactant Derived from 3α,12α-Dihydroxy-5β-cholan-24-amine (Steroid Residue) and Ethylenediamintetraacetic Acid (Spacer). *Langmuir* **2008**, *24*, 6060–6066. [CrossRef] [PubMed]
22. Davis, A.P. Bile acid scaffolds in supramolecular chemistry: The interplay of design and synthesis. *Molecules* **2007**, *12*, 2106–2122. [CrossRef] [PubMed]
23. Svobodova, H.; Noponen, V.; Kolehmainen, E.; Sievaenen, E. Recent advances in steroidal supramolecular gels. *RSC Adv.* **2012**, *2*, 4985–5007. [CrossRef]
24. Newkome, G.R.; Shreiner, C. Dendrimers Derived from 1→3 Branching Motifs. *Chem. Rev.* **2010**, *110*, 6338–6442. [CrossRef] [PubMed]
25. Zhao, Y.; Cho, H.; Widanapathirana, L.; Zhang, S. Conformationally Controlled Oligocholate Membrane Transporters: Learning through Water Play. *Acc. Chem. Res.* **2013**, *46*, 2763–2772. [CrossRef] [PubMed]
26. Holm, R.; Mullertz, A.; Mu, H. Bile salts and their importance for drug absorption. *Int. J. Pharm.* **2013**, *453*, 4–55. [CrossRef] [PubMed]
27. Brotherhood, P.R.; Davis, A.P. Steroid-based anion receptors and transporters. *Chem. Soc. Rev.* **2010**, *39*, 3633–3647. [CrossRef] [PubMed]
28. Savage, P.B. Cationic steroid antibiotics. *Curr. Med. Chem. Anti-Infect. Agents* **2002**, *1*, 293–304. [CrossRef]
29. Giglio, E. Inclusion compounds of deoxycholic acid. In *Inclusion Compounds*; Academic Press: London, UK, 1984; Volume 2, pp. 207–229.
30. Miyata, M.; Sada, K. Deoxycholic acid and related hosts. In *Comprehensive Supramolecular Chemistry*; MacNicol, D.D., Toda, F., Bishop, R., Eds.; Elsevier: Oxford, UK, 1996; Volume 6, pp. 147–176.
31. Campanelli, A.R.; de Sanctis, S.C.; Giglio, E.; Viorel Pavel, N.; Quagliata, C. From crystal to micelle: A new approach to the micellar structure. *J. Incl. Phenom. Macrocycl. Chem.* **1989**, *7*, 391–400. [CrossRef]

32. Froemming, K.H.; Sandmann, R. New preparative method for gastric juice-resistant forms at active substances. *Arch. Pharm.* **1970**, *303*, 71–378.
33. Sada, K.; Sugahara, M.; Kato, K.; Miyata, M. Controlled Expansion of a Molecular Cavity in a Steroid Host Compound. *J. Am. Chem. Soc.* **2001**, *123*, 4386–4392. [CrossRef] [PubMed]
34. Sugahara, M.; Sada, K.; Miyata, M. A robust structural motif in inclusion crystals of nor-bile acids. *Chem. Commun.* **1999**, 293–294. [CrossRef]
35. Sugahara, M.; Sada, K.; Hirose, J.; Miyata, M. Inclusion abilities of bile acids with different side chain length. *Mol. Cryst. Liq. Cryst.* **2001**, *356*, 155–162. [CrossRef]
36. Hishikawa, Y.; Aoki, Y.; Sada, K.; Miyata, M. Selective inclusion phenomena in lithocholamide crystal lattices; design of bilayered assemblies through ladder-type hydrogen bonding network. *Chem. Lett.* **1998**, *27*, 1289–1290. [CrossRef]
37. Kato, K.; Tohnai, N.; Miyata, M. Hierarchical prediction process of cholic acid crystal structures based on characteristic helical assemblies. *Mol. Cryst. Liq. Cryst.* **2005**, *440*, 125–132. [CrossRef]
38. Hisaki, I.; Tohnai, N.; Miyata, M. Supramolecular tilt chirality in crystals of steroids and alkaloids. *Chirality* **2008**, *20*, 330–336. [CrossRef] [PubMed]
39. Hisaki, I.; Shizuki, N.; Sasaki, T.; Ito, Y.; Tohnai, N.; Miyata, M. Handedness Determination of 21 Helical Motifs and Hierarchical Analysis of Crystal Structures Based on the Motifs: The Case of Cinchona Alkaloid Derivatives. *Cryst. Growth Des.* **2010**, *10*, 5262–5269. [CrossRef]
40. Hisaki, I.; Sasaki, T.; Tohnai, N.; Miyata, M. Supramolecular-tilt-chirality on twofold helical assemblies. *Chem. Eur. J.* **2012**, *18*, 10066–10073. [CrossRef] [PubMed]
41. Tanaka, A.; Inoue, K.; Hisaki, I.; Tohnai, N.; Miyata, M.; Matsumoto, A. Supramolecular chirality in layered crystals of achiral ammonium salts and fatty acids: A hierarchical interpretation. *Angew. Chem. Int. Ed.* **2006**, *45*, 4142–4145. [CrossRef] [PubMed]
42. Tanaka, A.; Hisaki, I.; Tohnai, N.; Miyata, M. Supramolecular tilt chirality derived from symmetrical benzene molecules: Handedness of the 21 helical assembly. *Chem. Asian J.* **2007**, *2*, 230–238. [CrossRef] [PubMed]
43. Miyata, M.; Tohnai, N.; Hisaki, I. Supramolecular chirality in crystalline assemblies of bile acids and their derivatives; three-axial, tilt, helical, and bundle chirality. *Molecules* **2007**, *12*, 1973–2000. [CrossRef] [PubMed]
44. Hisaki, I.; Watabe, T.; Kogami, Y.; Tohnai, N.; Miyata, M. 21 Helical assemblies of cinchona alkaloids in crystals: Definition of their handedness based on the molecular tilt. *Chem. Lett.* **2006**, *35*, 1274–1275. [CrossRef]
45. Miyata, M.; Shibakami, M.; Takemoto, K. Optical resolution of lactones by an inclusion method using cholic acid as the host. *J. Chem. Soc. Chem. Commun.* **1988**, 655–656. [CrossRef]
46. Miki, K.; Kasai, N.; Shibakami, M.; Takemoto, K.; Miyata, M. New Chiral Recognition Ability of a Steroidal Bile Acid; Direct Evidence for Efficient Optical Resolution of Racemic Lactones by Cholic Acid Inclusion Crystals. *J. Chem. Soc. Chem. Commun.* **1991**, 1757–1759. [CrossRef]
47. Bortolini, O.; Fantin, G.; Fogagnolo, M.; Medici, A.; Pedrini, P. Optical resolution of sulfoxides by inclusion in host dehydrocholic acid. *Chem. Commun.* **2000**, 365–366. [CrossRef]
48. Bortolini, O.; Fantin, G.; Fogagnolo, M.; Medici, A.; Pedrini, P. Resolution of unfunctionalized epoxides by cholic acid inclusion compounds. *Chem. Lett.* **2000**, 1246–1247. [CrossRef]
49. Bortolini, O.; Fantin, G.; Fogagnolo, M. Bile acid derivatives as enantiodifferentiating host molecules in inclusion processes. *Chirality* **2005**, *17*, 121–130. [CrossRef] [PubMed]
50. Bortolini, O.; Fantin, G.; Fogagnolo, M.; Maietti, S. Resolution of organic racemates via host-guest enantioselective inclusion complexation in bile acid derivatives. *ARKIVOC* **2006**, *2006*, 40–48. [CrossRef]
51. Meijide, F.; Trillo, J.V.; de Frutos, S.; Galantini, L.; Pavel, N.V.; Soto, V.H.; Jover, A.; Vázquez Tato, J. Crystal structure of head-to-head dimers of cholic and deoxycholic acid derivatives with different symmetric bridges. *Steroids* **2013**, *78*, 247–254. [CrossRef] [PubMed]
52. Meijide, F.; Trillo, J.V.; de Frutos, S.; Gancedo, C.; Soto, V.H.; Galantini, L.; Jover, A.; Vázquez Tato, J. Crystal structure of a head-to-head bis(cholic)-urea dimer. In Proceedings of the 18th International Electronic Conference on Synthetic Organic Chemistry, 1–30 November 2014.
53. Anelli, P.L.; Lattuada, L.; Uggeri, F. One-pot Mitsunobu-Staudinger preparation of 3-aminocholan-24-oic acid esters from 3-hydroxycholan-24-oic acid esters. *Synth. Commun.* **1998**, *28*, 109–117. [CrossRef]
54. Hwang, I.H.; Lee, S.J.; Chang, J.Y. Supramolecular Discotic Liquid Crystals from Wedge-Shaped Diacetylenes and Their Polymerization. *J. Polym. Sci. A* **2003**, *41*, 1881–1891. [CrossRef]

55. Nakano, K.; Sada, K.; Miyata, M. Inclusion Compounds of Cholic Acid with Various Hydrocarbons and the Crystal Structure of a 1:1 Complex of Cholic Acid and Benzene. *Chem. Lett.* **1994**, *23*, 137–140. [CrossRef]
56. Yoswathananont, N.; Sadaand, K.; Miyata, M. Inclusion compounds of cholic acid with large aliphatic alcohols. *Mol. Cryst. Liq. Cryst.* **2002**, *389*, 47–51. [CrossRef]
57. Altona, C.; Geise, H.J.; Romers, C. Conformation of nonaromatic ring compounds. XXV. Geometry and conformation of ring D in some steroids from x-ray structure determinations. *Tetrahedron* **1968**, *24*, 13–32. [CrossRef]
58. Reger, D.L.; Horger, J.J.; Smith, M.D.; Long, G.J.; Grandjean, F. Homochiral, Helical Supramolecular Metal-Organic Frameworks Organized by Strong π...π Stacking Interactions: Single-Crystal to Single-Crystal Transformations in Closely Packed Solids. *Inorg. Chem.* **2011**, *50*, 686–704. [CrossRef] [PubMed]
59. Chung, D.D.L. Review graphite. *J. Mater. Sci.* **2002**, *37*, 1475–1489. [CrossRef]
60. Alvarez, S. A cartography of the van der Waals territories. *Dalton Trans.* **2013**, *42*, 8617–8636. [CrossRef] [PubMed]
61. Shikii, K.; Sakamoto, S.; Seki, H.; Utsumi, H.; Yamaguchi, K. Narcissistic aggregation of steroid compounds in diluted solution elucidated by CSI-MS, PFG NMR and X-ray analysis. *Tetrahedron* **2004**, *60*, 3487–3492. [CrossRef]
62. Shieh, H.-S.; Hoard, L.G.; Nordman, C.E. The structure of cholesterol. *Acta Cryst.* **1981**, *B37*, 1538–1543. [CrossRef]
63. Giglio, E.; Quagliata, C. Side-chain and ring D conformation in cholanic acids. *Acta Cryst.* **1975**, *B31*, 743–746. [CrossRef]